Validation of Geant4 low energy physics models against electron energy deposition and backscattering data

Anton Lechner, *Student Member, IEEE,* Maria Grazia Pia and Manju Sudhakar

***Abstract*—A comprehensive and systematic validation of Geant4 electromagnetic physics models, relevant to the low-energy domain ($\leq$ 1 MeV), was performed. Considering different materials, the energy deposition pattern and backscattering are investigated for electron beams of varying energies and incident angles. The obtained simulation results are compared against high-precision experimental data. The study provides an useful guidance for low-energy physics simulation applications based on the Geant4 toolkit.**

***Index Terms*—Geant4, validation, low-energy electrons.**

I. Introduction

THE electron transport in matter is fundamental to simulation applications involving electrons either as primary particles or secondary products; thus a detailed understanding of the accuracy of relevant models with respect to experimental data is of great importance for Monte Carlo developers and users. Systematic investigations of the simulation accuracy over a variety of conditions, covering different materials and energies, allow to obtain a global picture of the abilities and shortcomings of physics models.

The study presented here addresses a comprehensive validation of Geant4 [1], [2] electron energy deposition and backscattering simulations for a variety of target materials, incident angles and beam energies in the low-energy range ($\leq$1 MeV). Simulation results are compared against experimental data in [3], [4]. Earlier attempts exist to validate Geant4 against these measurements, but they consider only a limited subset of the available experimental data (see e.g. [5], [6]). The current validation project has as its primary objective the coverage of the complete experimental data set. An initial, still significant collection of results is presented, focusing on Geant4 library-based interactions models (see section II).

II. Geant4 electromagnetic physics

The current validation process examines the accuracy achievable with Geant4 physics models describing the electromagnetic interactions of electrons and photons. The Geant4 toolkit offers alternative physics process implementations applicable to simulations in the low-energy domain, which are contained in the *Low-Energy* [7] and in the *Standard* [8] electromagnetic packages. The relevant physics processes for electrons and photons and the corresponding implementations are summarized in Table I.

The *Low-Energy* package contains two alternative approaches for both electrons and photons: one relying on the parametrization of data libraries (EEDL [9] for electrons and EPDL [10] for photons) and the second utilizing analytical descriptions originally developed for the Penelope Monte Carlo code [11], [12]. Only results corresponding to the EEDL and EPDL parametrizations are presented in this paper.

A unique implementation of the multiple-scattering process exists in Geant4, which is part of the *Standard* package; this process is used in all the simulations described here.

III. Experimental data

The experimental data considered for the radiation study derive from [3] and [4]. The first reference includes a comprehensive collection of energy deposition measurements from incident electrons as a function of penetration depth in various targets, while the latter one provides a variety of experimental electron energy and charge albedos. Both data sets cover different target materials, spanning a wide range in atomic number (from beryllium to uranium). The measured data sets were originally intented for validating the TIGER code [13]. The uncertainty in the dose deposition is $<$2.2% [3].

For both experimental setups, calorimetric measurement techniques were applied to determine the physical observables under investigation:

- *Longitudinal energy delivery pattern.* To measure the energy deposition at a specified distance from the target surface, a calorimeter foil was placed between a front layer and a "semi-infinite" backward layer, i.e. a slab thicker than the range of most electrons. The calorimeter was made of the same material as the entire target configuration.
  For a given front slab, the measurement depth was determined as the slabs' thickness plus half the calorimeter thickness. Measurements were performed for different thicknesses of the front layers.
- *Backscattering.* The fractions of energy and charge backscattered from the target surface were determined indirectly by measuring the energy deposition and the current in a calorimeter. The albedos were then obtained by taking the complement, where for the energy albedos a

Manuscript received November 23, 2007.

A. Lechner is with the Atomic Institute of the Austrian Universities, Vienna University of Technology, Vienna, Austria and CERN, Geneva, Switzerland.

M. G. Pia is with INFN Sezione di Genova, Via Dodecaneso 33, I-16146 Genova, Italy (phone: +39 010 3536420, fax: +39 010 313358, e-mail: MariaGrazia.Pia@ge.infn.it).

M. Sudhakar is with the ISRO Satellite Centre, Bangalore, India.

TABLE I
ELECTROMAGNETIC PROCESSES IN GEANT4 FOR ELECTRONS AND PHOTONS

Package	**Low-Energy package**		**Standard package**
Model type	Library-based (Livermore)	Penelope-like	
Electrons			
Ionisation	G4LowEnergyIonisation	G4PenelopeIonisation	G4eIonisation
Bremsstrahlung	G4LowEnergyBremsstrahlung	G4PenelopeBremsstrahlung	G4eBremsstrahlung
Multiple-Scattering	-	-	G4MultipleScattering
Photons			
Photoelectric effect	G4LowEnergyPhotoelectric	G4PenelopePhotoelectric	G4PhotoElectricEffect
Compton scattering	G4LowEnergyCompton	G4PenelopeCompton	G4ComptonScattering
Rayleigh scattering	G4LowEnergyRayleigh	G4PenelopeRayleigh	-
Conversion	G4LowEnergyGammaConversion	G4PenelopeGammaConversion	G4GammaConversion

theoretical correction was applied considering the energy escape due to Bremsstrahlung photons leaving the target. More detailed descriptions of the setup and the measurement techniques can be found in [3], [4].

IV. SIMULATION SETUP

The data sets in [3] and [4] respectively derive from two experimental setups that partly differ in their components, but share major features. This facilitated the development of a simulation application which reproduces the measurement conditions of both experiments.

The energy spectrum of primary electrons was modeled as Gaussian curve, where sigma was taken to be the error associated with the measurement of the beam energy specified in [3], [4].

The physics processes activated in the simulations were the library-based models contained in the *Low-Energy* package and the multiple-scattering model of the *Standard* package (see Table I).

The target consisted of a cylinder and was defined as a sensitive detector; the energy deposition was scored in slabs placed inside the target. Albedos were calculated by keeping track of the particle and energy flux through the target surfaces.

An important simulation parameter is the upper size limit for steps a particle can take along its track, particulary if the spatial resolution of computed quantities like the energy deposition is investigated. An adequate choice for the maximum step size is a size length comparable to the thickness of the scoring slabs. The considered bin sizes were $\sim$0.001 mm for lower beam energies and $\sim$0.015 mm for beams of 1 MeV; thus the maximum step size was set to 0.001 mm for all simulation runs.

A further point of interest within the scope of the validation study is the threshold for producing secondary particles. The library-based models in the *Low-Energy* package allow for a lower production threshold of 250 eV.

V. RESULTS

The simulation results presented in the following were obtained with Geant4 version 9.0-p01; in a few cases simulations were also performed with version 8.1-p02 to study possible effects of the evolution of simulation models. If not explicitly specified, the results apply to a production threshold of 250 eV for electrons.

TABLE II
CONTINUOUS SLOWING DOWN APPROXIMATION RANGE FOR DIFFERENT MATERIALS AND BEAM ENERGIES (DATA TAKEN FROM [3])

Material	**Energy (MeV)**	**Range (g/cm2)**
Aluminium	0.521	0.234
	1.033	0.569
Iron	0.500	0.249
	1.000	0.606
Copper	0.300	0.125
	0.500	0.258
Molybdenum	0.500	0.281
	1.000	0.673
Tantalum	0.500	0.325
	1.000	0.763

A. Energy deposition pattern in homogeneous targets

To unify the data representation of results for different materials, the penetration depth is expressed as a fraction of a mean range, which is taken to be the continuous slowing down approximation (CSDA) range of the primary electrons. Table II summarizes the CSDA ranges [3] for the materials and beam configurations considered in the following subsections.

1) Energy deposition in different materials: Fig. 1 - 5 show the energy deposition per unit length as a function of depth for homogeneous targets of aluminium, iron, copper, molybdenum and tantalum. For each material curves are presented for primary beam energies of 0.3 MeV and 1.0 MeV, except for copper where the shown energy deposition pattern corresponds to 0.3 MeV and 0.5 MeV beams.

For both beam energies, the simulation results generally agree well with the experimental data and no significant systematic deviations between simulated and measured curves are observed. Particulary, in the tail region Geant4 reproduces the experimental values within a 2% level, except for a 1.0 MeV beam incident on iron, where larger differences occur.

The peak height of curves corresponding to a 1.0 MeV beam is slightly underestimated in the simulation. As is observed in the Fig. 4(b) and 5(b), this effect increases with the atomic number of the target material.

As indicated by the bars shown in the plots, the experimental calorimeter thickness is large compared to the variations in the energy distribution pattern in case of 0.3 MeV electrons incident on iron, copper and tantalum. Hence, the resolution of the measured energy deposition must be taken into account when interpreting the agreement between the simulated and experimental curves.

2) Effects due to production threshold: Fig. 6 shows the longitudinal energy distributions obtained with different secondary production thresholds. The considered target material is molybdenum, and the investigated beam energies are 0.3 MeV and 1.0 MeV, respectively. Simulation results are presented corresponding to the extreme cases where

- no secondaries are produced (i.e. the production threshold was greater than the beam energy),
- the lowest recommended limit for the low-energy parametrized physics models is applied (250 eV).

As is demonstrated in Figure 6, the choice of the production threshold significantly influences the peak height. Comparison against experimental data shows that the simulation utilizing the lower threshold is closer to the experimental values for a beam energy of 0.3 MeV, while the curve associated with a 1MeV beam is better reproduced by applying a high threshold. Similar effects are also observed for other materials.

3) Effect of angle of incidence: Fig. 7 shows the energy deposition pattern inside targets for beams having an incident angle of 60° with respect to the surface normal. The curves correspond to electrons of 0.3 MeV and 1.0 MeV impinging on aluminium and molybdenum, respectively. The simulation results well reproduce the experimental data; in most cases a better agreement with experimental data is observed at 60° incidence with respect to normal incidence: this hints to effects due to multiple scattering, that modulate the fraction of electrons releasing energy inside or outside the target.

4) Effects due to changes in multiple scattering: A set of simulations was performed with Geant4 version 8.1-p02 (see Fig. 1 - 5). The implementation of the low-energy parametrized processes listed in Table I is identical in 8.1-p02 and 9.0-p01, while the implementation of the multiple scattering algorithm differs. Consequently, deviations experienced in the energy deposition pattern are to be ascribed to the changes in the multiple-scattering model.

The simulation results associated with the two Geant4 versions exhibit significant differences, especially for lighter materials. The largest deviations are experienced for aluminium, and are of the same order of magnitude as the differences between simulation and experimental data. As shown in Figure 1, the changes in the multiple-scattering model primarily affect the peak region. For target materials with higher Z, like for molybdenum or tantalum, the results associated with Geant4 8.1-p02 and 9.0-p01 are not subject to large differences. Further investigation is currently in progress to evaluate the effects of the evolution of the multiple-scattering algorithm over the latest Geant4 versions.

B. Backscattering

Fig. 8 - 10 show the fraction of energy backscattered from a beryllium, aluminium and titanium target. Results are presented as a function of the incident angle; for each material different beam energies are investigated.

As indicated in the figures, a good agreement between experimental and simulation data is observed for aluminium and tantalum for all considered combinations of beam energy and incident angle. Similar results were achieved for other materials with an atomic number higher than aluminium.

In case of electrons with an energy of 0.109 MeV impinging on beryllium, Geant4 slightly overestimates the measured values; for this setup experimental data is only available for incident angles of 31° and 46° (see Fig. 8). The simulation results for a beryllium target show a better performance, if the energy is increased to 0.314 MeV: the backscattered energy fractions are well reproduced, except for the largest considered angle of incidence, where the experimental value is again overestimated. Investigation concerning backscattering effects for materials with low atomic number are currently in progress.

VI. Conclusions

A systematic validation study of Geant4 low-energy physics models for the electromagnetic interactions of electrons and photons was performed. Results associated with the parametrization models in the *Low-Energy* package were presented.

For both considered quantities, energy deposition and backscattering, the study demonstrates that a good agreement between experimental data and simulation data can be achieved over a large range of materials. Further investigations are currently in progress to analyse in detail the behaviour of all available low-energy electromagnetic models in Geant4.

References

[1] S. Agostinelli et al., "Geant4 - a simulation toolkit", *Nucl. Instrum. Meth. A*, vol. 506, no. 3, pp. 250-303, 2003.

[2] J. Allison et al., "Geant4 Developments and Applications", *IEEE Trans. Nucl. Sci.*, vol. 53, no. 1, pp. 270-278, 2006.

[3] G.J. Lockwood et al., "Calorimetric Measurement of Electron Energy Deposition in Extented Media - Theory vs Experiment", SAND79-0414 UC-34a, 1987.

[4] G.J. Lockwood et al., "Electron Energy and Charge Albedos - Calorimetric Measurement vs Monte Carlo Theory", SAND80-1968 UC-34a, 1987.

[5] O. Kadri et al., "Geant4 simulation of electron energy deposition in extented media", *Nucl. Instrum. Meth. B*, vol. 258, no. 2, pp. 381-387, 2007.

[6] J.F. Carrier, L. Archambault and L.Beaulieu, "Validation of GEANT4, an object-oriented Monte Carlo toolkit, for simulations in medical physics", *Med. Phys.*, vol. 31, no. 3, pp. 484-492, 2004.

[7] J. Apostolakis, S. Giani, M. Maire, P. Nieminen, M.G. Pia, L. Urban, "Geant4 low energy electromagnetic models for electrons and photons", *INFN/AE-99/18*, Frascati, 1999.

[8] H. Burkhardt et al., "Geant4 Standard Electromagnetic Package", in *Proc. 2005 Conf. on Monte Carlo Method: Versatility Unbounded in a Dynamic Computing World*, American Nuclear Society, Illinois, USA, 2005.

[9] S. T. Perkins et al., "Tables and Graphs of Electron-Interaction Cross Sections from 10 eV to 100 GeV Derived from the LLNL Evaluated Electron Data Library (EEDL)", UCRL-50400 Vol. 31, 1997.

[10] D. Cullen et al., "EPDL97, the Evaluated Photon Data Library", UCRL-50400, Vol. 6, Rev. 5, 1997.

[11] J. Baro, J. Sempau, J. M. Fernández-Varea, and F. Salvat, "PENELOPE, an algorithm for Monte Carlo simulation of the penetration and energy loss of electrons and positrons in matter", *Nucl. Instrum. Meth. B*, vol. 100, no. 1, pp. 31-46, 1995.

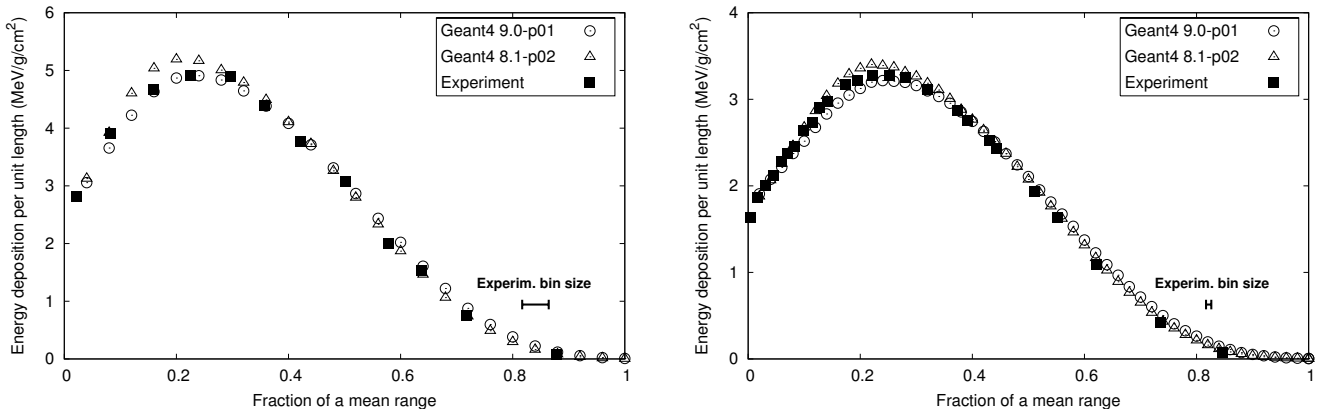

Fig. 1. Spatial energy deposition pattern along the beam axis in an aluminium target for an e^- beam with a primary energy of (a) 0.314 MeV and (b) 1.033 MeV. The simulation results obtained with the Geant4 versions 8.1p02 and 9.0p01, respectively, are compared against experimentally measured values [3].

[12] F. Salvat, J. M. Fernndez-Varea, and J. Sempau, "PENELOPE-2006: A Code System for Monte Carlo Simulation of Electron and Photon Transport", Nuclear Energy Agency Workshop Proceedings, Barcelona, Spain, Jul. 2006.

[13] J.A. Halbleib, Sr., and W.H. Vandevender, *Nucl. Sci. Eng.*, 57, 94, 1975.

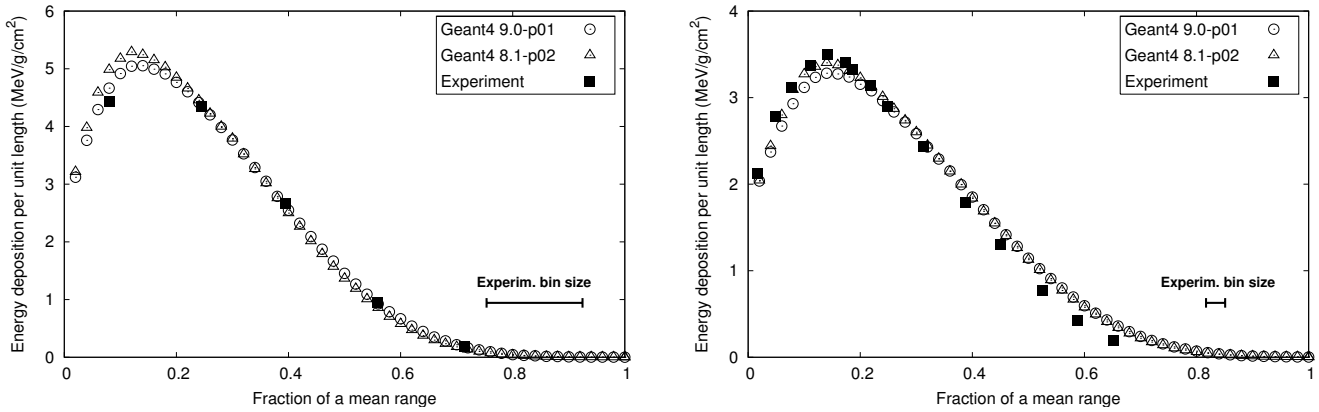

(a) (b)

Fig. 2. Spatial energy deposition pattern along the beam axis in an iron target for an e^- beam with a primary energy of (a) 0.3 MeV and (b) 1.0 MeV. The simulation results obtained with the Geant4 versions 8.1p02 and 9.0p01, respectively, are compared against experimentally measured values [3].

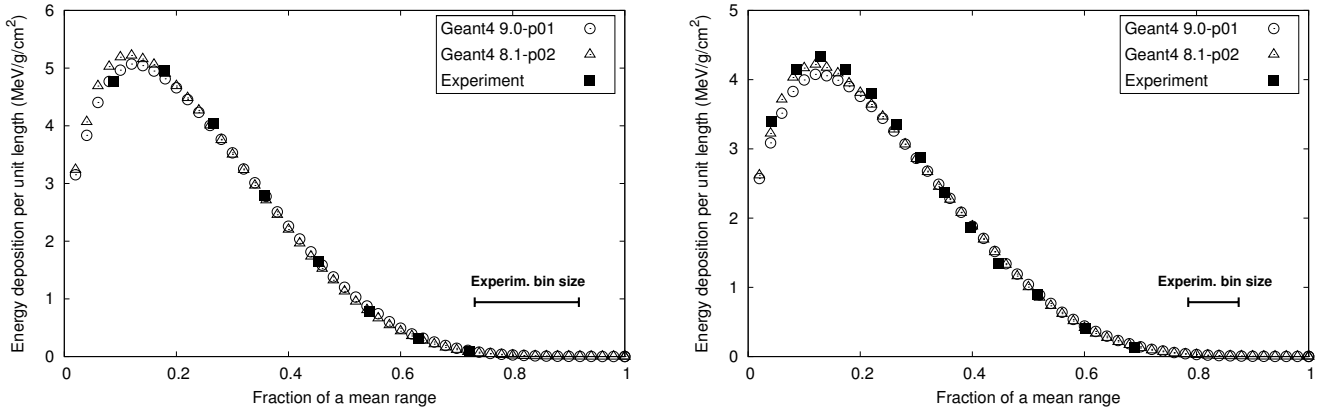

(a) (b)

Fig. 3. Spatial energy deposition pattern along the beam axis in a copper target for an e^- beam with a primary energy of (a) 0.3 MeV and (b) 0.5 MeV. The simulation results obtained with the Geant4 versions 8.1p02 and 9.0p01, respectively, are compared against experimentally measured values [3].

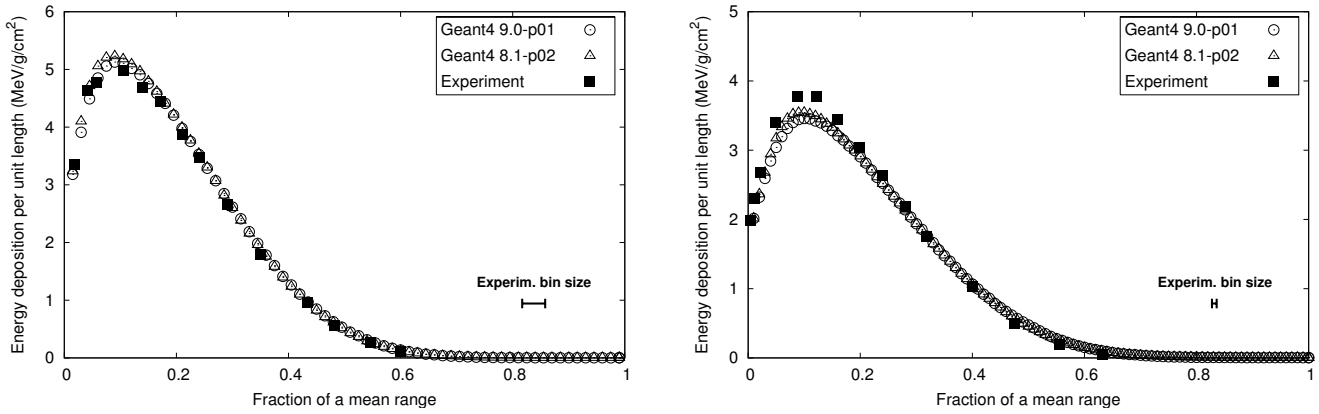

(a) (b)

Fig. 4. Spatial energy deposition pattern along the beam axis in a molybdenum target for an e^- beam with a primary energy of (a) 0.3 MeV and (b) 1.0 MeV. The simulation results obtained with the Geant4 versions 8.1p02 and 9.0p01, respectively, are compared against experimentally measured values [3].

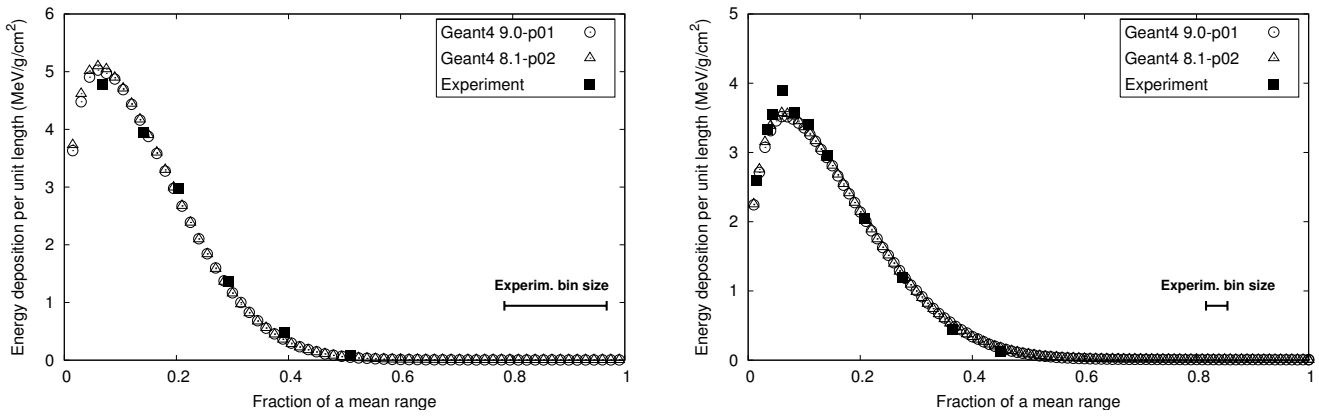

Fig. 5. Spatial energy deposition pattern along the beam axis in a tantalum target for an e^- beam with a primary energy of (a) 0.3 MeV and (b) 1.0 MeV. The simulation results obtained with the Geant4 versions 8.1p02 and 9.0p01, respectively, are compared against experimentally measured values [3].

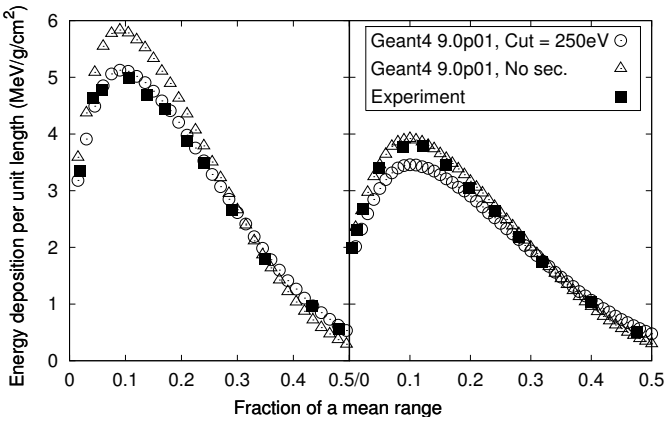

Fig. 6. Spatial energy deposition pattern along the beam axis in a molybdenum target for e^- beams with primary energies of 0.3 MeV (plot on the left) and 1.0 MeV (right plot). Simulation results obtained with different production thresholds are compared against experimental data. The simulations are based on Geant4 version 9.0-p01.

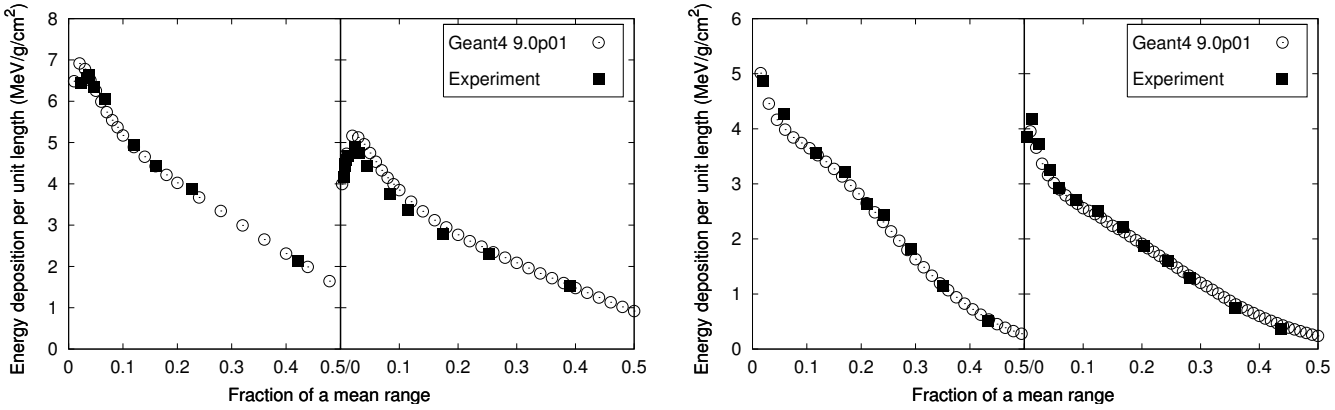

Fig. 7. Spatial energy deposition pattern along the axis normal to the target surface for e^- beams having an incident angle of 60°. Results are shown for (a) an aluminium and (b) a molybdenum target. The curves in figure (a) apply to primary beam energies of 0.314 MeV (left curve) and 1.033 MeV (right curve), respectively, while the curves in figure (b) correspond to energies of 0.3 MeV (left curve) and 1.0 MeV (right curve). The simulation results obtained with the Geant4 9.0p01 are compared against experimentally measured values [3].

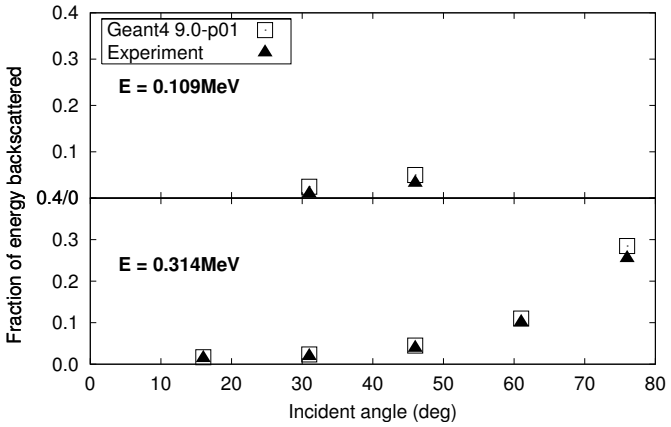

Fig. 8. Fraction of energy backscattered from a beryllium target.

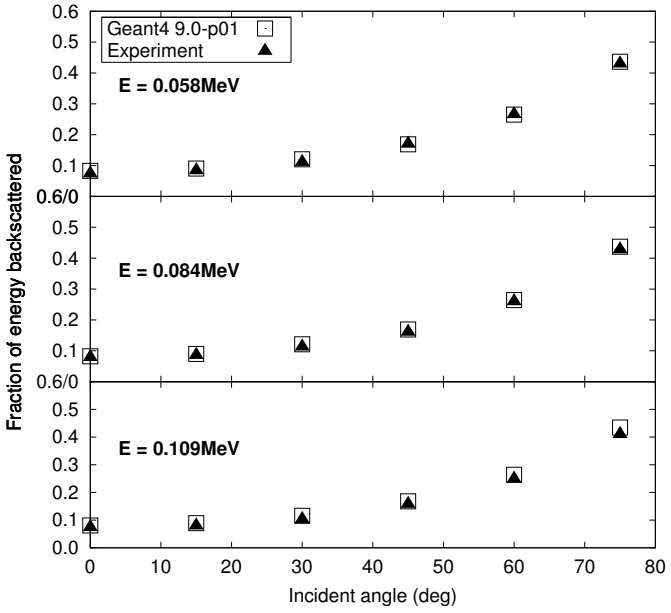

Fig. 9. Fraction of energy backscattered from an aluminium target.

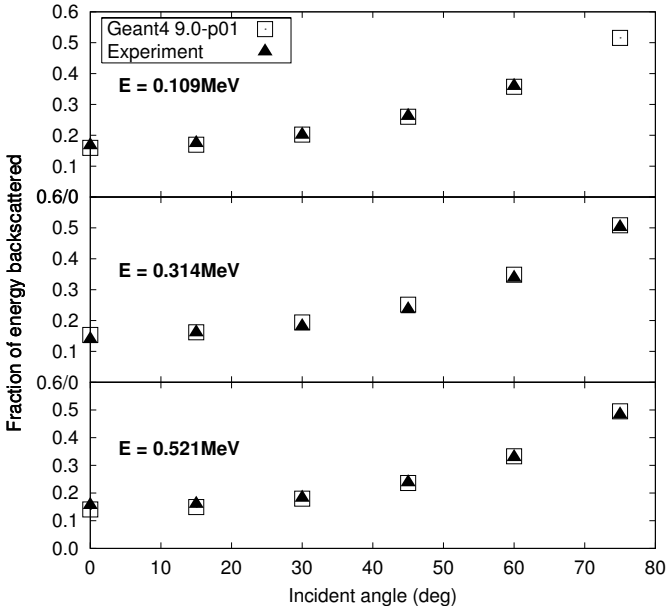

Fig. 10. Fraction of energy backscattered from a titanium target.